

Communication

# Surface Plasmon Resonance Biosensors with Magnetic Sandwich Hybrids for Signal Amplification

Ting Sun <sup>1,2</sup>, Mengyao Li <sup>2</sup>, Feng Zhao <sup>1,\*</sup> and Lin Liu <sup>2,\*</sup> 

<sup>1</sup> Key Laboratory of Functional Organic Molecule, School of Chemistry and Materials Science, Guizhou Integrated Research Center of Polymer Electromagnetic Materials, Guizhou Education University, Guiyang 550018, China; sunt725726@163.com

<sup>2</sup> College of Chemistry and Chemical Engineering, Anyang Normal University, Anyang 455000, China; 19837235165@163.com

\* Correspondence: zhaofeng327@163.com (F.Z.); liulin@aynu.edu.cn (L.L.)

**Abstract:** The conventional signal amplification strategies for surface plasmon resonance (SPR) biosensors involve the immobilization of receptors, the capture of target analytes and their recognition by signal reporters. Such strategies work at the expense of simplicity, rapidity and real-time measurement of SPR biosensors. Herein, we proposed a one-step, real-time method for the design of SPR biosensors by integrating magnetic preconcentration and separation. The target analytes were captured by the receptor-modified magnetic nanoparticles (MNPs), and then the biotinylated recognition elements were attached to the analyte-bound MNPs to form a sandwich structure. The sandwich hybrids were directly delivered to the neutravidin-modified SPR fluidic channel. The MNPs hybrids were captured by the chip through the neutravidin–biotin interaction, resulting in an enhanced SPR signal. Two SPR biosensors have been constructed for the detection of target DNA and beta-amyloid peptides with high sensitivity and selectivity. This work, integrating the advantages of one-step, real-time detection, multiple signal amplification and magnetic preconcentration, should be valuable for the detection of small molecules and ultra-low concentrations of analytes.

**Keywords:** surface plasmon resonance; biosensors; magnetic preconcentration; signal amplification



**Citation:** Sun, T.; Li, M.; Zhao, F.; Liu, L. Surface Plasmon Resonance Biosensors with Magnetic Sandwich Hybrids for Signal Amplification. *Biosensors* **2022**, *12*, 554. <https://doi.org/10.3390/bios12080554>

Received: 20 June 2022

Accepted: 20 July 2022

Published: 22 July 2022

**Publisher's Note:** MDPI stays neutral with regard to jurisdictional claims in published maps and institutional affiliations.



**Copyright:** © 2022 by the authors. Licensee MDPI, Basel, Switzerland. This article is an open access article distributed under the terms and conditions of the Creative Commons Attribution (CC BY) license (<https://creativecommons.org/licenses/by/4.0/>).

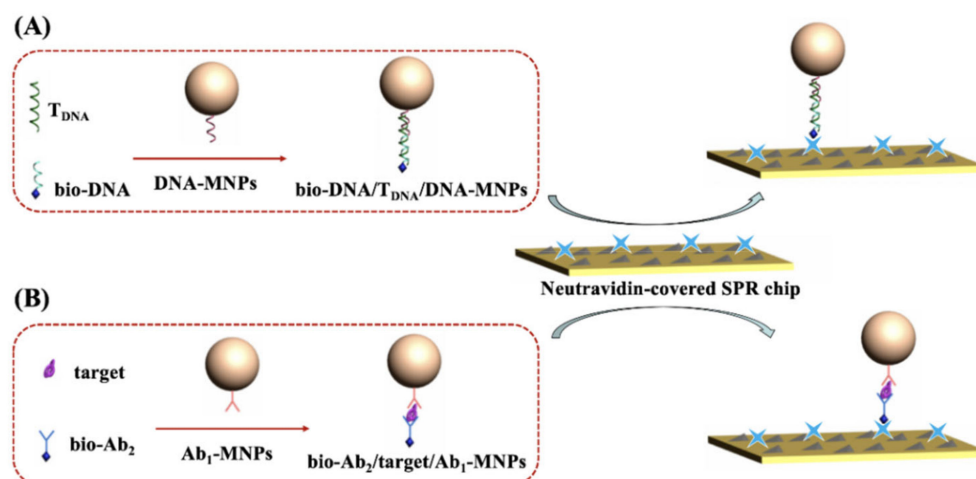
## 1. Introduction

Surface plasmon resonance (SPR) biosensors have been used for the real-time detection of different classes of biomarkers with the advantages of simple operation, rapid response and high selectivity. However, traditional SPR sensors are less sensitive for the direct detection of small molecules (<8 kDa) or ultra-low concentrations (1 pM) of analytes based on the change in refractive index or thickness near metal surfaces [1,2]. In view of this, many efforts have been made to improve the sensitivity of SPR biosensors using secondary signal amplification with gold nanomaterials, magnetic nanoparticles and biomacromolecules [3–12]. The targets can be determined with a competitive (signal-off) or sandwich-like (signal-on) format. In contrast to the signal-off assay, the signal-on sandwich assay exhibits higher sensitivity because of the low background signal [13]. In this method, antibodies or other receptors are usually anchored on the surface of an SPR chip for the capture of target analytes [14,15]. Then, the recognition element-modified biomacromolecules or nanomaterials with large molecular weight, large size or high refractive index are delivered onto the chip's surface to amplify the SPR signal. The secondary signal amplification can improve the sensitivity and avoid the influence of other components in biological fluids. However, these advantages come at the expense of simplicity, rapidity and real-time measurement due to a greater number of steps in the SPR analysis process [13]. Moreover, the storage of receptor-modified chips requires harsh conditions because of the limited stability of receptors such as antibodies under non-physiological conditions and high temperature [16]. Thus, it is of great significance to develop a general SPR biosensor

for the detection of small molecules and ultra-low concentrations of analytes by integrating the advantages of one-step, real-time detection and multiple signal amplification.

Magnetic nanoparticles (MNPs) provide a feasible solution to the persistent challenges arising from the sensitivity and nonspecific adsorption of the preconcentration and separation of target analytes. Recently, some innovative sensing concepts involving MNP technologies have been reported for the ultra-sensitive detection of cells, nucleic acids, proteins and small biomolecules [17]. Usually, the target analytes are captured by the MNPs modified with specific receptors and then collected with a magnetic field. The analyte-bound MNPs can be brought to the sensor surface or can be removed from the sample and re-dispersed in solution. A good example of the concept is the electrochemical magneto-biosensor [18–20], in which the analyte-bound MNPs are collected by a magnetic electrode to produce a strong electrochemical signal. Alternately, the MNPs can also be captured by nucleic acid- or antibody-modified solid surfaces to produce optical signals [6,7,21–25]. For instance, MNPs have been successfully used to enhance the SPR signal due to their advantages of high molecular mass, high refractive index, low production cost and easy synthesis through hydrothermal and co-precipitative methods [4,26–32]. However, there are still some challenges related to the real-time SPR assays using MNP technologies [33]. For instance, the chips need to be covered with specific receptors through appropriate modification methods and the storage of the sensor chips requires harsh conditions. The capture of analyte-bound MNPs through the hybridization reaction or antibody–antigen interaction requires a long hybridization time and a low flow rate. Moreover, the immobilization of receptors on the chip surface may produce a steric hindrance for the capture of analyte-bound MNPs at the solid–liquid interface [34]. Therefore, new MNP-based SPR biosensors are still desired to simplify the detection procedure, shorten the analysis time and improve the detection efficiency.

Apart from the hybridization reaction and antibody–antigen interaction, the avidin–biotin system has been extensively used in biomedical analysis. Avidin and its analogues, including streptavidin (SA) or neutravidin (NA), modified on a solid surface show high stability, easy controllability and excellent flexibility [35–37]. Many SA or NA-labeled signal tags or solid supports and biotinylated reagents are commercially available. Herein, we proposed an MNP-based strategy for the design of one-step, real-time SPR biosensors based on the avidin–biotin interaction. As shown in Scheme 1, the MNPs were modified with the receptors such as DNA or antibodies for the preconcentration and separation of target analytes through the hybridization reaction or antibody–antigen interaction. Then, the biotinylated recognition elements (DNA or second antibody) were attached onto the MNPs' surface by binding to the targets via the same interactions. The NA-covered chips were utilized to capture the sandwich hybrids formed between biotinylated recognition elements, analytes and receptor-modified MNPs. The attachment of such sandwich hybrids is dependent upon the NA–biotin interaction, and the number of hybrids is proportional to the concentration of targets. Thus, the analysis of targets was converted to the direct detection of sandwich hybrids, significantly amplifying the signal due to the large size of MNPs and antibodies. Moreover, the magnetic preconcentration and separation can eliminate the nonspecific adsorption of other components in biological samples onto the chip surface, thus remarkably improving the sensitivity and selectivity. The dissociation constant between NA and biotin is in the order of  $10^{14} \text{ M}^{-1}$ . Such a powerful and specific interaction will facilitate the capture of the hybrids at a faster flow rate, thereby shortening the analysis time and decreasing the nonspecific interactions.



**Scheme 1.** Schematic representation of DNA biosensor (A) and immunosensor (B) by directly injecting the sandwich hybrids onto the NA-covered SPR chip.

## 2. Materials and Methods

### 2.1. Chemicals and Materials

Carboxylated MNPs with a diameter of ~100 nm were ordered from Ruixi Biotech. Co., Ltd. (Xi'an, China). Free and FITC-labeled NA proteins were provided by Thermo Fisher Scientific (Shanghai, China). DNA, avidin and glutathione (GSH) were obtained from Sangon Biotech. Co., Ltd. (Shanghai, China). Beta-amyloid peptides, human serum protein (HSA), beta-secretase, bovine serum protein (BSA), 1-ethyl-3-[3-dimethylaminopropyl]carbodiimide hydrochloride (EDC), N-hydroxysulfosuccinimide (NHS) and 1,1,1,3,3,3-hexafluoro-2-propanol (HFIP) were acquired from Sigma-Aldrich (Shanghai, China). The sequences of DNA are 5'-NH<sub>2</sub>-TTT TTG TAA AAC GAC GGC CAG-3' (capture probe DNA), 5'-TAG GAA TAG TTA TAA CTG GCC GTC GTT TTA C-3' (target DNA, T<sub>DNA</sub>) and 5'-TTA TAA CTA TTC CTA-biotin-3' (bio-DNA). Monoclonal antibody (Ab<sub>1</sub>) and biotinylated second antibody (bio-Ab<sub>2</sub>) specific to A $\beta$ <sub>40</sub> were obtained from Covance Inc. (Dedham, MA, USA). A $\beta$ <sub>16</sub> was provided by China Peptide Co., Ltd. (Shanghai, China). Other reagents were ordered from Aladdin Reagent Co., Ltd. (Shanghai, China). The peptide of A $\beta$ <sub>40</sub> was dissolved in HFIP solution and then reconstituted in NaOH to a concentration of 1 mM. Before its use, the peptide was diluted with 10 mM phosphate buffer (pH 7.2) to a desired concentration.

### 2.2. Functionalization of MNPs

Carboxylated MNPs were modified with capture probe DNA or antibody (Ab<sub>1</sub>) by the EDC/NHS-activated covalent coupling reaction. Briefly, 5 mg of MNPs was dispersed in 2 mL of phosphate buffer solution containing 50 mM EDC and 10 mM NHS for 15 min. After the carboxylic groups on the nanoparticle surface were activated, the MNPs were washed with water and re-dispersed in 2 mL of phosphate buffer solution containing 0.2  $\mu$ M NH<sub>2</sub>-DNA or 50  $\mu$ g/mL of Ab<sub>1</sub>. After incubation for 2 h, the unreacted activated carboxylic groups on MNPs were blocked by incubation with 10 mM ethanolamine for 30 min. After being rinsed with water to remove the unreacted substances, the resulting DNA-MNPs or Ab<sub>1</sub>-MNPs were dispersed in 2 mL of phosphate buffer containing 10  $\mu$ M BSA and stored at 4 °C for use. The change in the zeta potential of MNPs induced by surface modification was monitored on a zeta potential analyzer (Nano ZS, Malvern Company, Worcestershire, UK).

### 2.3. Preparation of SPR Chips

The gold chips were cleaned by a hydrogen flame and then incubated with 1  $\mu$ M NA in carbonate buffer (pH 10) for 2 h. NA proteins were capped on the gold surface through

the hydrophobic and Au–S interactions [38]. After washing the chip with buffer to remove the unbound NA proteins, the unreacted gold surface was sealed by incubation of the chip with 10  $\mu\text{M}$  BSA and 100  $\mu\text{M}$  GSH for 30 min. The resulting NA/BSA/GSH-covered chips were thoroughly washed and stored at 4  $^{\circ}\text{C}$  for use.

#### 2.4. SPR Analysis

Before the SPR assay, 900  $\mu\text{L}$  of target DNA ( $T_{\text{DNA}}$ ) or  $A\beta_{40}$  sample at a given concentration was spiked with 50  $\mu\text{L}$  of 5 nM biotinylated DNA (bio-DNA) or bio- $Ab_2$  at 37  $^{\circ}\text{C}$ . Then, 50  $\mu\text{L}$  of DNA-MNPs or  $Ab_1$ -MNPs suspension was added to the sample. After incubation for 1 h, the MNPs were rinsed three times with a magnetic field and then dispersed in 0.5 mL of phosphate buffer. For the real-time measurement, the NA/BSA/GSH-covered chip was fixed on a BI-SPR 3000 instrument (Biosensing Instrument Inc., Tempe, AZ, USA). When a stable baseline was attained, the resulting bio-DNA/ $T_{\text{DNA}}$ /DNA-MNPs or bio- $Ab_2$ / $A\beta_{40}$ / $Ab_1$ -MNPs hybrids were delivered to the fluidic channel by a syringe pump, and the signal was recorded according to the change in the SPR refractive index.

### 3. Results and Discussion

#### 3.1. Principle and Feasibility

To demonstrate the practicability of the strategy, a DNA biosensor was constructed by the formation of sandwich bio-DNA/ $T_{\text{DNA}}$ /DNA-MNPs hybrids. The principle of the method was depicted in Scheme 1A. The capture probe DNA was immobilized on the surface of MNPs to generate DNA-MNPs. When the  $T_{\text{DNA}}$  was hybridized with bio-DNA and the capture probe DNA on MNPs, the sandwich bio-DNA/ $T_{\text{DNA}}$ /DNA-MNPs hybrids were formed. The excessive bio-DNA and other substances in the samples were then removed, and the  $T_{\text{DNA}}$  targets were concentrated with a magnetic field. The re-dispersed sandwich hybrids were then delivered to the fluidic channel and captured by NA proteins modified on the chip, thus producing an enhanced SPR signal due to the large molecular mass and high refractive index of MNPs. In this work, NA-covered gold chips were used to capture the biotinylated probe. To prove that NA can be anchored on the gold surface, the chip incubated with FITC-NA instead of NA was characterized by fluorescence microscope. As shown in Figure 1A, a green, fluorescent image was observed on the chip coated with FITC-NA/BSA/GSH, while the BSA/GSH-covered chip was black. This is indicative of the successful attachment of NA proteins on the chip surface. Moreover, the successful modification of DNA onto the surface of MNPs was confirmed by monitoring the change in the zeta potential. The zeta potential of MNPs changed from  $-11.2$  to  $-13.7$  mV after the modification of the capture probe DNA. After the hybridization reaction, the zeta potential became  $-18.2$  mV. The increase in the negative charge is indicative of the formation of bio-DNA/ $T_{\text{DNA}}$ /DNA-MNPs hybrids.

As expected, injection of the bio-DNA/ $T_{\text{DNA}}$ /DNA-MNPs hybrids into the sensor channel caused a significant change in the SPR dip shift (curve a in Figure 1B). However, a negligible change was observed when injecting DNA-MNPs (curve b) or  $T_{\text{DNA}}$ /DNA-MNPs (curve c) to the channel. In the absence of  $T_{\text{DNA}}$ , the signal was close to the background level, indicating that there is no nonspecific adsorption between DNA-MNPs and the sensor chip. A control experiment was conducted by injecting the bio-DNA/ $T_{\text{DNA}}$ /DNA-MNPs hybrids into BSA/GSH instead of the NA/BSA/GSH-modified chip (curve d). Consequently, no significant change in the SPR dip shift was observed. Therefore, the change in curve a can be attributed to the  $T_{\text{DNA}}$ -triggered hybridization reaction and the NA-biotin interaction. In addition, a smaller SPR dip shift was attained when injecting bio-DNA/ $T_{\text{DNA}}$ /DNA hybrids into the NA/BSA/GSH-covered chip (curve e), indicating that the SPR signal can be greatly intensified by MNPs (curve a).

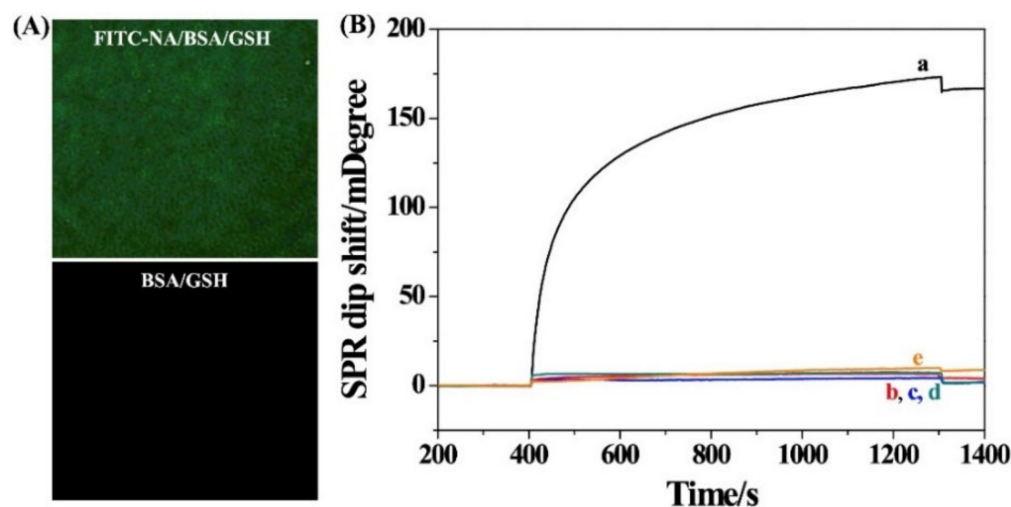


**Figure 1.** (A) Fluorescence microscopy images of the FITC-NA/BSA/GSH and BSA/GSH-modified chips. (B) SPR sensorgrams for injection of different hybrids onto the NA/BSA/GSH-modified chip: curve a, bio-DNA/ $T_{DNA}$ /DNA-MNPs; curve b, DNA-MNPs; curve c,  $T_{DNA}$ /DNA-MNPs; curve e, bio-DNA/ $T_{DNA}$ /DNA. Curve d corresponds to that for injection of bio-DNA/ $T_{DNA}$ /DNA-MNPs onto the BSA/GSH-modified chip. The concentration of  $T_{DNA}$  was 1.5 pM.

### 3.2. Sensitivity for DNA Detection

After the successful preparation of the SPR biosensor,  $T_{DNA}$  at different concentrations was analyzed. Figure 2A shows the SPR curves obtained when the DNA-MNPs and bio-DNA were incubated with different concentrations of  $T_{DNA}$ . The SPR dip shift increased with the increase in  $T_{DNA}$  concentration, further demonstrating that the signal change resulted from the binding of sandwich hybrids. A good linear relationship between the  $T_{DNA}$  concentration and the SPR dip shift was attained (Figure 2B). The linear equation can be expressed as  $\theta = 0.10[T_{DNA}]$  (fM) + 6.54 in the concentration range of 1–2000 fM (the inset). The high sensitivity with a detection limit of 1 fM can be attributed to the signal amplification of MNPs and the magnetic preconcentration of  $T_{DNA}$ . Moreover, since the hybridization reaction was performed in the solution and the NA–biotin system shows a strong interaction, the real-time SPR assays have been achieved at a fast flow rate, shortening the analysis time and decreasing the nonspecific interactions.

### 3.3. Immunoassays of $A\beta_{40}$

Immunoassays with the signal amplification of nanomaterials, including MNPs, have been widely applied in clinical analysis, food safety control, environmental monitoring and so on [39,40]. To demonstrate the applications of the sensing strategy in different fields, an SPR immunosensor was constructed and used for the detection of amyloid peptide  $A\beta_{40}$ . As shown in Scheme 1B, the  $Ab_1$ -MNPs were used to capture  $A\beta_{40}$  and bio- $Ab_2$  through the specific antigen–antibody recognition. After the formation of sandwich bio- $Ab_2$ / $A\beta_{40}$ / $Ab_1$ -MNPs, the hybrids were separated and then delivered to the NA/BSA/GSH-covered chip. As shown in Figure 3, a negligible change in the SPR dip shift was observed when injecting  $Ab_1$ -MNPs (curve a) or  $A\beta_{40}$ / $Ab_1$ -MNPs (curve b) into the sensor chip. However, a significant change was attained after injection of bio- $Ab_2$ / $A\beta_{40}$ / $Ab_1$ -MNPs to the chip surface (curve c). The value is much higher than that by injecting bio- $Ab_2$ / $A\beta_{40}$ / $Ab_1$  into the chip (curve d), indicating that MNPs indeed enhanced the SPR signal due to the high molecular mass and high refractive index.

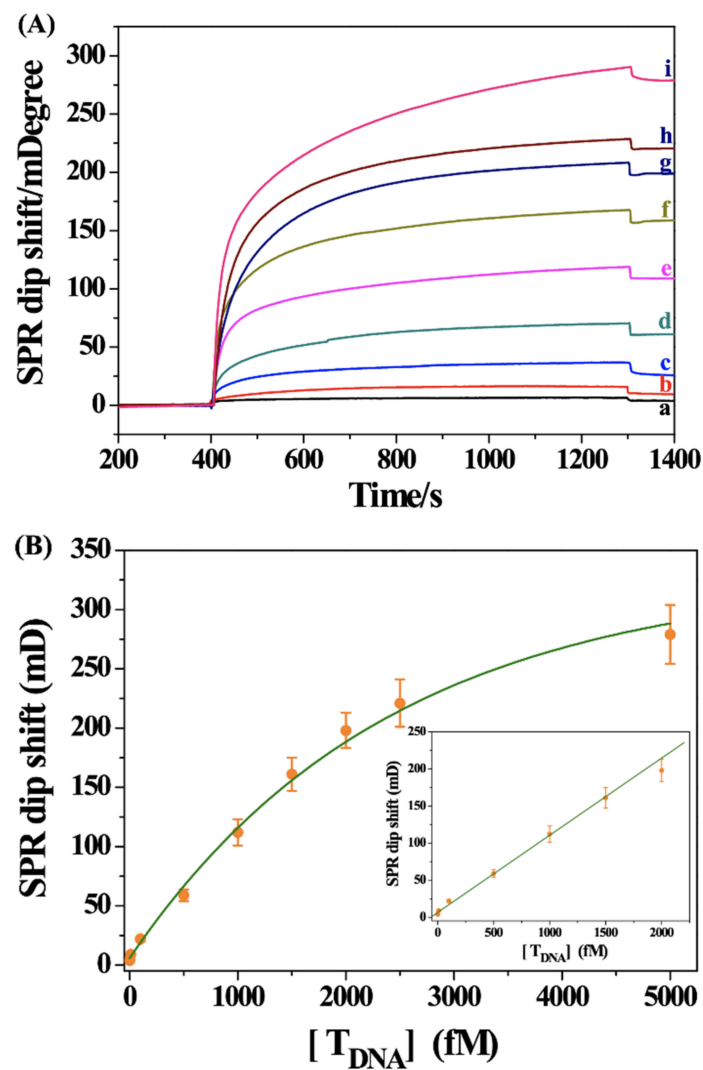


**Figure 2.** (A) SPR sensorgrams for the detection of different concentrations of  $T_{DNA}$  (a~i: 1, 10, 100, 500, 1000, 1500, 2000, 2500 and 5000 fM). (B) Dependence of SPR signal on  $T_{DNA}$  concentration. The inset shows the linear portion of the fitting curve.

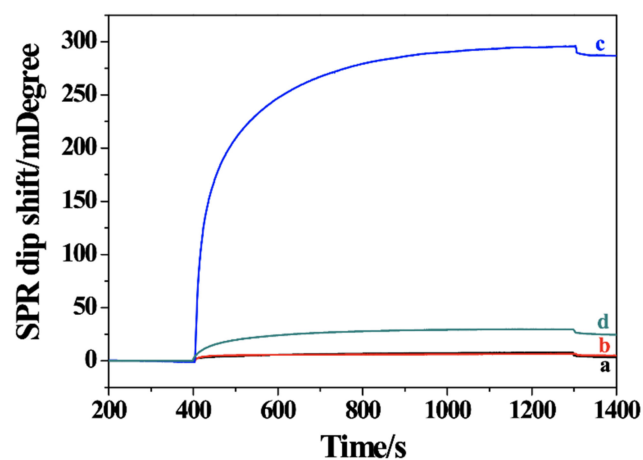


**Figure 3.** SPR sensorgrams for injection of Ab<sub>1</sub>-MNPs (curve a), A $\beta_{40}$ /Ab<sub>1</sub>-MNPs (curve b), bio-Ab<sub>2</sub>/A $\beta_{40}$ /Ab<sub>1</sub>-MNPs (curve c) and bio-Ab<sub>2</sub>/A $\beta_{40}$ /Ab<sub>1</sub> (curve d) into the NA/BSA/GSH-modified chip. The concentration of A $\beta_{40}$  was 2.5 pM.

The analytical performance for the detection of  $A\beta_{40}$  was investigated by determining different concentrations of  $A\beta_{40}$ . As shown in Figure 4A, the SPR dip shift increased gradually when the  $Ab_1$ -MNPs were incubated with increasing concentrations of  $A\beta_{40}$  in the presence of  $bio-Ab_2$ , indicating that the formation of sandwich hybrids was dependent upon the concentration of  $A\beta_{40}$ . The method allowed for the detection of  $A\beta_{40}$  with a linear range of 10–2500 fM (Figure 4B). The linear equation between the  $A\beta_{40}$  concentration and the SPR dip shift was found to be  $\theta = 0.11[A\beta_{40}]$  (fM) + 3.34. The detection limit was estimated to be 5 fM, which is lower than that achieved by other methods (Table 1). The high sensitivity can be attributed to the multiple signal amplification by antibodies and MNPs and the magnetic preconcentration. Thus, the one-step, real-time assay was particularly suitable for the detection of small molecules and ultra-low concentrations of analytes. Plasmonic nanoparticles (e.g., Au and Ag) exhibit strong optical resonance for visible and near-infrared wavelengths. We believe that the analytical performance, including detection limit and linear range, could be further improved by using magneto-plasmonic nanostructures as the signal labels [23,26–28,41].

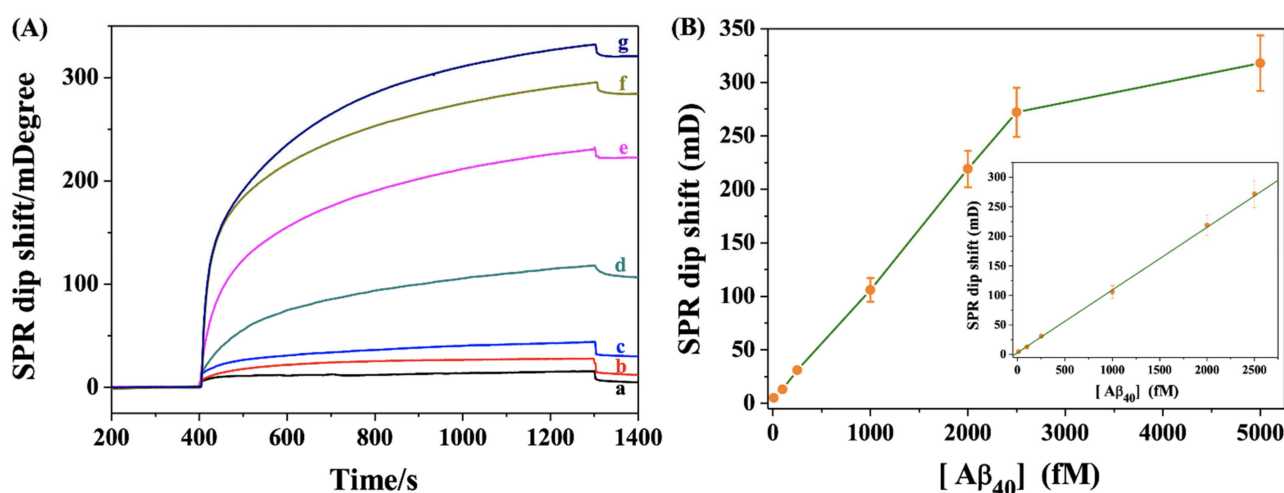


**Figure 4.** (A) SPR sensorgrams for the detection of different concentrations of  $A\beta_{40}$  (a–g: 10, 100, 250, 1000, 2000, 2500 and 5000 fM). (B) Dependence of SPR signal on  $A\beta_{40}$  concentration. The inset shows the linear portion of the fitting curve.

**Table 1.** An overview of different sandwich biosensors for  $A\beta_{40}$  detection.

Method	Signal Label	Linear Range	Detection Limit	Ref.
DPV	AuNPs/HRP	0.1–50 nM	28 pM	[42]
DPV	AuNPs	0.2–40 nM	50 pM	[43]
ECL	Au@NiFe MOFs	22 fM–11 nM	3 fM	[44]
ECL	Ru@MOFs	2.2 fM–110 nM	0.85 fM	[45]
LSPR	AuNPs	10 fM–100 nM	34.9 fM	[46]
SPR	SA- $Ab_2$	10 pM–150 nM	20 pM	[47]
SPR	$bio-Ab_2/Ab_1$ -MNPs	10–2500 fM	5 fM	This work

Abbreviations: DPV, differential pulse voltammetry; ECL, electrochemiluminescence; LSPR, localized surface plasmon resonance; SPR, surface plasmon resonance; AuNPs, gold nanoparticles; HRP, horseradish peroxidase; MOFs, metal–organic frameworks.

### 3.4. Selectivity for $A\beta_{40}$ Detection

In addition to the high sensitivity, the specific antigen–antibody recognition promised excellent selectivity of the biosensor. Figure 5 shows the results for analysis of different samples, including other  $A\beta$  fragments ( $A\beta_{16}$  and  $A\beta_{42}$ ), serum protein HSA, beta-secretase and biotin-binding protein avidin. When the  $Ab_1$ -MNPs and  $bio-Ab_2$  were incubated with  $A\beta_{16}$ ,  $A\beta_{42}$ , HSA, beta-secretase and avidin, even at a higher concentration, no

significant change in the SPR dip shift was observed (bars 1–5). The result indicated that the biosensor exhibited high selectivity. We also found that the coexistence of avidin in the  $A\beta_{40}$  sample decreased the SPR signal for the detection of  $A\beta_{40}$  (cf. bars 6 and 7). The result is understandable since avidin can bind to bio- $Ab_2/A\beta_{40}/Ab_1$ -MNPs through the avidin–biotin interaction, thus preventing the attachment of the hybrids to the chip’s surface. However, the interference can be readily eliminated by two-step magnetic separation. As expected, a high SPR signal was attained when the  $Ab_1$ -MNPs were incubated with the mixture of  $A\beta_{40}$  and avidin and then separated by a magnetic field, followed by incubation of the  $A\beta_{40}/Ab_1$ -MNPs with bio- $Ab_2$  and separated by a magnetic field again (bar 8). The result not only demonstrated that the signal was enhanced by MNPs, but it also indicated that the capture of the  $Ab_1$ -MNPs was dependent upon the antigen–antibody and NA–biotin interactions. Moreover, the high sensitivity and magnetic preconcentration are conducive to improving the selectivity because the interference from other components in complex, real samples can be decreased by sample dilution and magnetic separation. Thus, the SPR immunosensor should be an excellent candidate for the detection of MNPs-based extracted products.

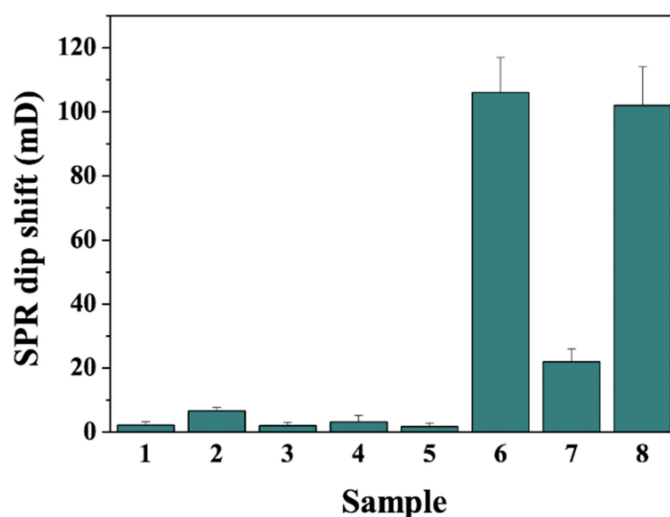


**Figure 5.** Selectivity of the method toward 1 nM  $A\beta_{16}$  (bar 1), 1 nM  $A\beta_{42}$  (bar 2), 10 ng/mL HSA (bar 3), 1 nM beta-secretase (bar 4), 5 nM avidin (bar 5), 1 pM  $A\beta_{40}$  (bar 6) and the mixture of 1 nM avidin and 1 pM  $A\beta_{40}$  by one-step (bar 7) or two-step (bar 8) magnetic separation.

#### 4. Conclusions

In summary, we proposed a general strategy for the design of SPR biosensors by integration of magnetic preconcentration. The signal was amplified by the integrated sandwich hybrids composed of recognition elements, target analytes, receptors and MNPs. The performance of the method was evaluated by detecting DNA and  $A\beta_{40}$  in which the sandwich hybrids were directly delivered to the sensor surface. The target concentration, down to 1 fM for DNA or 10 fM for  $A\beta_{40}$ , can be readily measured. The method exhibits the merits of rapid response, real-time measurement, high sensitivity and excellent specificity. Since SA and NA proteins have high thermal stability and excellent biocompatibility and many biotinylated recognition elements are commercially available, the method would explore new applications of SPR biosensors, especially for the detection of small molecules and ultra-low concentrations of analytes. Moreover, novel electrochemical and optical technologies can be developed based on the magnetic preconcentration and avidin–biotin interaction.

**Author Contributions:** Conceptualization, L.L. and F.Z.; methodology, T.S.; investigation, T.S. and M.L.; writing—original draft preparation, T.S.; writing—review and editing, L.L.; project administration, F.Z.; funding acquisition, L.L. and F.Z. All authors have read and agreed to the published version of the manuscript.

**Funding:** This research was funded by the Science and Technology Foundation of Guizhou Province (No. QKHJC-ZK[2022]332), the Reward and Subsidy Fund Project of Guizhou Education University, the Ministry of Science and Technology of the People's Republic of China and the National Natural Science Foundation of China (No. 2021GZJ003), the Guizhou Education University Doctor Program (No. 2021BS028) and the Guizhou University Integrated Research Platform (No. QJHKY(2020)008).

**Institutional Review Board Statement:** Not applicable.

**Informed Consent Statement:** Not applicable.

**Data Availability Statement:** Not applicable.

**Conflicts of Interest:** The authors declare no conflict of interest.

## References

1. Tabasi, O.; Falamaki, C. Recent advancements in the methodologies applied for the sensitivity enhancement of surface plasmon resonance sensors. *Anal. Methods* **2018**, *10*, 3906. [[CrossRef](#)]
2. Chang, C.C. Recent advancements in aptamer-based surface plasmon resonance biosensing strategies. *Biosensors* **2021**, *11*, 233. [[CrossRef](#)]
3. Zeng, S.; Baillargeat, D.; Ho, H.-P.; Yong, K.-T. Nanomaterials enhanced surface plasmon resonance for biological and chemical sensing applications. *Chem. Soc. Rev.* **2014**, *43*, 3426. [[CrossRef](#)]
4. Teramura, Y.; Arima, Y.; Iwata, H. Surface plasmon resonance-based highly sensitive immunosensing for brain natriuretic peptide using nanobeads for signal amplification. *Anal. Biochem.* **2006**, *357*, 208. [[CrossRef](#)]
5. Huang, Y.; Sun, T.; Liu, L.; Xia, N.; Zhao, Y.; Yi, X. Surface plasmon resonance biosensor for the detection of miRNAs by combining the advantages of homogeneous reaction and heterogeneous detection. *Talanta* **2021**, *234*, 122622. [[CrossRef](#)]
6. Wang, J.; Munir, A.; Zhu, Z.; Zhou, H.S. Magnetic nanoparticle enhanced surface plasmon resonance sensing and its application for the ultrasensitive detection of magnetic nanoparticle-enriched small molecules. *Anal. Chem.* **2010**, *82*, 6782. [[CrossRef](#)]
7. Wang, Y.; Dostalek, J.; Knoll, W. Magnetic nanoparticle-enhanced biosensor based on grating-coupled surface plasmon resonance. *Anal. Chem.* **2011**, *83*, 6202. [[CrossRef](#)]
8. Mitchell, J.S.; Wu, Y.; Cook, C.J.; Main, L. Sensitivity enhancement of surface plasmon resonance biosensing of small molecules. *Anal. Biochem.* **2005**, *343*, 125. [[CrossRef](#)]
9. Sun, T.; Zhang, Y.; Zhao, F.; Xia, N.; Liu, L. Self-assembled biotin-phenylalanine nanoparticles for the signal amplification of surface plasmon resonance biosensors. *Microchim. Acta* **2020**, *187*, 473. [[CrossRef](#)]
10. Prabowo, B.A.; Purwidyantri, A.; Liu, B.; Lai, H.C.; Liu, K.C. Gold nanoparticle-assisted plasmonic enhancement for DNA detection on a graphene-based portable surface plasmon resonance sensor. *Nanotechnology* **2021**, *32*, 095503. [[CrossRef](#)]
11. Mandala, S.H.S.; Liu, T.-J.; Chen, C.-M.; Liu, K.K.; Januar, M.; Chang, Y.-F.; Lai, C.-S.; Chang, K.-H.; Liu, K.-C. Enhanced plasmonic biosensor utilizing paired antibody and label-free Fe<sub>3</sub>O<sub>4</sub> nanoparticles for highly sensitive and selective detection of Parkinson's  $\alpha$ -synuclein in serum. *Biosensors* **2021**, *11*, 402. [[CrossRef](#)]
12. Lou, Z.; Han, H.; Zhou, M.; Wan, J.; Sun, Q.; Zhou, X.; Gu, N. Fabrication of magnetic conjugation clusters via intermolecular assembling for ultrasensitive surface plasmon resonance (SPR) detection in a wide range of concentrations. *Anal. Chem.* **2017**, *89*, 13472–13479. [[CrossRef](#)]
13. Masson, J.-F. Surface plasmon resonance clinical biosensors for medical diagnostics. *ACS Sens.* **2017**, *2*, 16. [[CrossRef](#)]
14. Sarcina, L.; Mangiatordi, G.F.; Torricelli, F.; Bollella, P.; Gounani, Z.; Österbacka, R.; Macchia, E.; Torsi, L. Surface Plasmon Resonance Assay for Label-Free and Selective Detection of HIV-1 p24 Protein. *Biosensors* **2021**, *11*, 180. [[CrossRef](#)]
15. Park, J.-H.; Cho, Y.-W.; Kim, T.-H. Recent advances in surface plasmon resonance sensors for sensitive optical detection of pathogens. *Biosensors* **2022**, *180*, 12. [[CrossRef](#)]
16. Mauriz, E. Low-fouling substrates for plasmonic sensing of circulating biomarkers in biological fluids. *Biosensors* **2020**, *10*, 63. [[CrossRef](#)]
17. Gloag, L.; Mehdipour, M.; Chen, D.; Tilley, R.D.; Gooding, J.J. Advances in the application of magnetic nanoparticles for sensing. *Adv. Mater.* **2019**, *31*, 1904385. [[CrossRef](#)]
18. Campuzano, S.; Torrente-Rodríguez, R.M.; López-Hernández, E.; Conzuelo, F.; Granados, R.; And, S.P.; Pingarrón, J.M. Rapid electrochemical assessment of tumor suppressor gene methylations in raw human serum and tumor cells and tissues using immunomagnetic beads and selective DNA hybridization. *Angew. Chem. Int. Ed.* **2014**, *53*, 6168. [[CrossRef](#)]
19. Tavallaie, R.; McCarroll, J.; Grand, M.L.; Ariotti, N.; Schuhmann, W.; Bakker, E.; Tilley, R.D.; Hibbert, D.B.; Kavallaris, M.; Gooding, J.J. Nucleic acid hybridization on an electrically reconfigurable network of gold-coated magnetic nanoparticles enables microRNA detection in blood. *Nat. Nanotechnol.* **2018**, *13*, 1066. [[CrossRef](#)]
20. Nemr, C.R.; Smith, S.J.; Liu, W.; Mephram, A.H.; Mohamadi, R.M.; Labib, M.; Kelley, S.O. Nanoparticle-mediated capture and electrochemical detection of methicillin-resistant *Staphylococcus aureus*. *Anal. Chem.* **2019**, *91*, 2847–2853. [[CrossRef](#)]
21. Soelberg, S.D.; Stevens, R.C.; Limaye, A.P.; Furlong, C.E. Surface plasmon resonance detection using antibody-linked magnetic nanoparticles for analyte capture, purification, concentration, and signal amplification. *Anal. Chem.* **2009**, *81*, 2357. [[CrossRef](#)]

22. Hill, H.D.; Mirkin, C.A. The bio-barcode assay for the detection of protein and nucleic acid targets using DTT-induced ligand exchange. *Nat. Protoc.* **2006**, *1*, 324. [[CrossRef](#)]
23. Philip, A.; Kumar, A.R. The performance enhancement of surface plasmon resonance optical sensors using nanomaterials: A review. *Coordin. Chem. Rev.* **2022**, *458*, 214424. [[CrossRef](#)]
24. Wang, L.; Lin, J. Recent advances on magnetic nanobead based biosensors: From separation to detection. *TrAC-Trend. Anal. Chem.* **2020**, *128*, 115915. [[CrossRef](#)]
25. Materón, E.M.; Miyazaki, C.M.; Carr, O.; Joshi, N.; Picciani, P.H.S.; Dalmaschio, C.J.; Davis, F.; Shimizu, F.M. Magnetic nanoparticles in biomedical applications: A review. *Appl. Surf. Sci. Adv.* **2021**, *6*, 100163. [[CrossRef](#)]
26. Wang, J.; Zhu, Z.; Munir, A.; Zhou, H.S. Fe<sub>3</sub>O<sub>4</sub> nanoparticles-enhanced SPR sensing for ultrasensitive sandwich bio-assay. *Talanta* **2011**, *84*, 783. [[CrossRef](#)]
27. Liang, R.-P.; Yao, G.-H.; Fan, L.-X.; Qiu, J.-D. Magnetic Fe<sub>3</sub>O<sub>4</sub>@Au composite-enhanced surface plasmon resonance for ultrasensitive detection of magnetic nanoparticle-enriched  $\alpha$ -fetoprotein. *Anal. Chim. Acta* **2012**, *737*, 22. [[CrossRef](#)]
28. Chen, H.; Qi, F.; Zhou, H.; Jia, S.; Gao, Y.; Koh, K.; Yin, Y. Fe<sub>3</sub>O<sub>4</sub>@Au nanoparticles as a means of signal enhancement in surface plasmon resonance spectroscopy for thrombin detection. *Sens. Actuat. B Chem.* **2015**, *212*, 505. [[CrossRef](#)]
29. Zou, F.; Wang, X.; Qi, F.; Koh, K.; Lee, J.; Zhou, H.; Chen, H. Magneto-plasmonic nanoparticles enhanced surface plasmon resonance TB sensor based on recombinant gold binding antibody. *Sens. Actuat. B Chem.* **2017**, *250*, 356. [[CrossRef](#)]
30. Jia, Y.; Peng, Y.; Bai, J.; Zhang, X.; Cui, Y.; Ning, B.; Cui, J.; Gao, Z. Magnetic nanoparticle enhanced surface plasmon resonance sensor for estradiol analysis. *Sens. Actuat. B Chem.* **2018**, *254*, 629. [[CrossRef](#)]
31. Reiner, A.T.; Ferrer, N.-G.; Venugopalan, P.; Lai, R.C.; Lim, S.K.; Dostálek, J. Magnetic nanoparticle-enhanced surface plasmon resonance biosensor for extracellular vesicle analysis. *Analyst* **2017**, *142*, 3913. [[CrossRef](#)] [[PubMed](#)]
32. Krishnan, S.; Mani, V.; Wasalathanthri, D.; Kumar, C.V.; Rusling, J.F. Attomolar detection of a cancer biomarker protein in aerum by surface plasmon resonance using superparamagnetic particle labels. *Angew. Chem. Int. Ed.* **2011**, *50*, 1175. [[CrossRef](#)] [[PubMed](#)]
33. Chang, Y.-F.; Chou, Y.-T.; Cheng, C.-Y.; Hsu, J.-F.; Su, L.-C.; Ho, J.A.A. Amplification-free detection of cytomegalovirus miRNA using a modification-free surface plasmon resonance biosensor. *Anal. Chem.* **2021**, *93*, 8002–8009. [[CrossRef](#)]
34. Wang, Y.; Partridge, A.; Wu, Y. Improving nanoparticle-enhanced surface plasmon resonance detection of small molecules by reducing steric hindrance via molecular linkers. *Talanta* **2019**, *198*, 350. [[CrossRef](#)]
35. Chen, Y.-H.; Gupta, N.K.; Huang, H.-J.; Lam, C.H.; Huang, C.-L.; Tan, K.-T. Affinity-switchable lateral flow assay. *Anal. Chem.* **2021**, *93*, 5556. [[CrossRef](#)] [[PubMed](#)]
36. Xia, N.; Sun, Z.; Ding, F.; Wang, Y.; Sun, W.; Liu, L. Protease biosensor by conversion of a homogeneous assay into a surface-tethered electrochemical analysis based on streptavidin–biotin interactions. *ACS Sens.* **2021**, *6*, 1166–1173. [[CrossRef](#)]
37. Xia, N.; Sun, T.; Liu, L.; Tian, L.; Sun, Z. Heterogeneous sensing of post-translational modification enzymes by integrating the advantage of homogeneous analysis. *Talanta* **2022**, *237*, 122949. [[CrossRef](#)]
38. Liu, X.; Wang, Y.; Chen, P.; Wang, Y.; Zhang, J.; Aili, D.; Liedberg, B. Biofunctionalized gold nanoparticles for colorimetric sensing of botulinum neurotoxin a light chain. *Anal. Chem.* **2014**, *86*, 2345. [[CrossRef](#)]
39. Farka, Z.K.; Juřík, T.S.; Kovář, D.; Trnková, L.E.; Sklaádal, P. Nanoparticle-based immunochemical biosensors and assays: Recent advances and challenges advances and challenges. *Chem. Rev.* **2017**, *117*, 9973–10042. [[CrossRef](#)]
40. Chiu, N.F.; Huang, T.Y.; Lai, H.C.; Liu, K.C. Graphene oxide-based SPR biosensor chip for immunoassay applications. *Nanoscale Res. Lett.* **2014**, *9*, 445. [[CrossRef](#)]
41. Bhatia, P.; Verma, S.S.; Sinha, M.M. Optical properties simulation of magneto-plasmonic alloys nanostructures. *Plasmonics* **2019**, *14*, 611. [[CrossRef](#)]
42. Yu, Y.; Sun, X.; Tang, D.; Li, C.; Zhang, L.; Nie, D.; Yin, X.; Shi, G. Gelsolin bound  $\beta$ -amyloid peptides (1–40/1–42): Electrochemical evaluation of levels of soluble peptide associated with Alzheimer’s disease. *Biosens. Bioelectron.* **2015**, *68*, 115. [[CrossRef](#)] [[PubMed](#)]
43. Yu, Y.; Zhang, L.; Li, C.; Sun, X.; Tang, D.; Shi, G. A method for evaluating the level of soluble  $\beta$ -amyloid (1–40/1–42) in Alzheimer’s disease based on the binding of gelsolin to  $\beta$ -amyloid peptides. *Angew. Chem. Int. Ed.* **2014**, *53*, 12832. [[CrossRef](#)] [[PubMed](#)]
44. Zhao, G.; Wang, Y.; Li, X.; Yue, Q.; Dong, X.; Du, B.; Cao, W.; Wei, Q. Dual-quenching electrochemiluminescence strategy based on three-dimensional metal–organic frameworks for ultrasensitive detection of amyloid- $\beta$ . *Anal. Chem.* **2019**, *91*, 1989–1996. [[CrossRef](#)] [[PubMed](#)]
45. Wang, Y.; Zhang, Y.; Sha, H.; Xiong, X.; Jia, N. Design and biosensing of a ratiometric electrochemiluminescence resonance energy transfer aptasensor between a g-C<sub>3</sub>N<sub>4</sub> nanosheet and Ru@MOF for amyloid- $\beta$  protein. *ACS Appl. Mater. Interfaces* **2019**, *11*, 36299–36306. [[CrossRef](#)]
46. Kim, H.; Lee, J.U.; Song, S.; Kim, S.; Sim, S.J. A shape-code nanoplasmonic biosensor for multiplex detection of Alzheimer’s disease biomarkers. *Biosens. Bioelectron.* **2018**, *101*, 96. [[CrossRef](#)]
47. Xia, N.; Liu, L.; Harrington, M.G.; Wang, J.; Zhou, F. Regenerable and simultaneous surface plasmon resonance detection of abeta(1–40) and abeta(1–42) peptides in cerebrospinal fluids with signal amplification by streptavidin conjugated to an N-terminus-specific antibody. *Anal. Chem.* **2010**, *82*, 10151. [[CrossRef](#)]